



OPEN ACCESS

EDITED BY

Tania F. De Koning-Ward, Deakin University, Australia

REVIEWED BY

Kristina E. M. Persson, Lund University, Sweden Daniel Kepple, Carolinas Healthcare System, United States

*CORRESPONDENCE

Markus Kalkum

mkalkum@coh.org

Manuel Alfonso Patarrovo

RECEIVED 22 July 2025 ACCEPTED 03 September 2025 PUBLISHED 25 September 2025

CITATION

Molina-Franky J, Röth D, Ararat-Sarria M, Patarroyo MA and Kalkum M (2025) The reticulocyte restriction: invasion ligand RBP1a of *Plasmodium vivax* targets human TfR1, prohibitin-2, and basigin. Front. Cell. Infect. Microbiol. 15:1671048. doi: 10.3389/fcimb.2025.1671048

© 2025 Molina-Franky, Röth, Ararat-Sarria, Patarrovo and Kalkum. This is an open-access article distributed under the terms of the Creative Commons Attribution License (CC BY). The use, distribution or reproduction in other forums is permitted, provided the original author(s) and the copyright owner(s) are credited and that the original publication in this journal is cited, in accordance with accepted academic practice. No use, distribution or reproduction is permitted which does not comply with these terms.

The reticulocyte restriction: invasion ligand RBP1a of Plasmodium vivax targets human TfR1, prohibitin-2, and basigin

Jessica Molina-Franky^{1,2,3,4}, Daniel Röth¹, Monica Ararat-Sarria 3,5, Manuel Alfonso Patarroyo 3,4,5,6* and Markus Kalkum^{1*}

¹Department of Immunology and Theranostics, Arthur Riggs Diabetes and Metabolism Research Institute, Beckman Research Institute of the City of Hope, Duarte, CA, United States, ²Global Scholars Program, Beckman Research Institute of the City of Hope, Duarte, CA, United States, ³Grupo de Investigación Básica en Biología Molecular e Inmunología (GIBBMI), Fundación Instituto de Inmunología de Colombia (FIDIC), Bogotá, Colombia, ⁴PhD Program in Biotechnology, Universidad Nacional de Colombia, Bogotá, Colombia, ⁵School of Medicine and Health Sciences, Universidad del Rosario, Bogotá, Colombia, ⁶Microbiology Department, Faculty of Medicine, Universidad Nacional de Colombia, Bogotá, Colombia

Introduction: Plasmodium vivax is the most widespread cause of malaria outside Africa. Developing effective controls is challenging because P. vivax exclusively invades reticulocytes, immature erythrocytes that are scarce and short-lived. This limits opportunities to culture the parasite and investigate the receptor-ligand interactions crucial for host cell invasion.

Methods: The erythroid cell lines JK-1 and BEL-A were evaluated in vitro as reticulocyte surrogates to assess their susceptibility to P. vivax invasion. Comparative membrane proteomics of these cell lines, reticulocytes, and mature erythrocytes were performed using quantitative liquid chromatography-mass spectrometry (LC-MS). Specific interactions between the parasite ligand PvRBP1a (residues 158-650) and candidate host receptors were identified by TurboID proximity labeling and validated through ELISA binding assays.

Results: We confirmed that the JK-1 cell line supports P. vivax invasion and demonstrated for the first time that BEL-A cells are similarly susceptible, establishing both as effective surrogate models. Membrane proteomics identified several receptor candidates potentially involved in selective host-cell entry. In addition to known receptors, including transferrin receptor protein 1 (TfR1/CD71), CD98hc, and basigin (BSG), novel receptor candidates such as prohibitin-2 (PHB2), CAT-1 (SLC7A1), ATB(0) (SLC1A5), CD36, integrin beta-1 (ITGB1), and metal transporter CNNM3 were discovered. Proximity labeling with a recombinant PvRBP1a (158-650)-TurboID fusion protein confirmed the known interactions with TfR1 and BSG, and additionally identified PHB2 as a novel

interacting partner. Notably, this is the first report implicating PHB2 as a coreceptor for *P. vivax* invasion.

Conclusion: Our findings provide novel insights into the molecular mechanisms underlying reticulocyte restriction in *P. vivax*. The JK-1 and BEL-A cell lines represent valuable platforms for dissecting receptor–ligand interactions during parasite invasion and for advancing the development of targeted therapeutic antimalarial strategies.

KEYWORDS

Plasmodium vivax, parasite invasion, erythroid cell lines, membrane proteomics, receptor-ligand interactions, LC-MS proteomics

1 Introduction

Malaria remains a major global health issue, with 263 million cases reported in 2023. *Plasmodium vivax*, one of the six humaninfecting *Plasmodium* species, is noteworthy for its global distribution. In the Americas, most malaria cases are due to *P. vivax* (72.1% in 2023) (World Health Organization, 2024). Its blood stage form, the merozoites, interact with red blood cell (RBC) receptors leading to RBC invasion (Gruszczyk et al., 2018a; Malleret et al., 2021; Molina-Franky et al., 2022). However, *P. vivax* exclusively infects reticulocytes (Malleret et al., 2015a), immature, short-lived precursors of erythrocytes, posing a significant challenge to research progress. In contrast, *P. falciparum* has been extensively researched due to the availability of a well-established *in vitro* culture system for over 40 years (Trager and Jensen, 1976). This critical disparity highlights the urgent need to develop alternative research models for *P. vivax*.

The mechanism of *P. vivax* reticulocyte invasion remains unclear. It was previously believed that *P. vivax* exclusively targeted reticulocytes through the Duffy antigen receptor for chemokines (DARC) and Duffy binding protein (PvDBP) interaction (Horuk et al., 1993), as individuals with the Fy(a-b-) mutation in West Africa were resistant to the infection. However, DARC is present on both reticulocytes and erythrocytes, and *P. vivax* infections have been documented in Duffy-negative populations (Ryan et al., 2006; Reyes et al., 2022; Picón-Jaimes et al., 2023).

Together with evidence from Duffy-negative infections, geographical variation among *P. vivax* isolates further supports the idea that invasion is not limited to a single pathway. Transcriptomic studies show that invasion-related genes such as *PvRBP1a*, *PvRBP2a*, and *PvRBP2b* are more highly expressed in Ethiopian and Cambodian isolates than in Brazilian isolates, while *PvDBP1* and *PvEBP/DBP2* are elevated in Cambodian parasites. These patterns suggest that *P. vivax* employs multiple, regionally adapted invasion strategies (Kepple et al., 2023). Among the most prominent candidates are the reticulocyte-binding protein (RBP) family, which may interact with transferrin

receptor 1 (TfR1) and CD98 heavy chain (SLC3A2), both of which are lost during the maturation of reticulocytes to erythrocytes (Galinski et al., 1992; Gruszczyk et al., 2018a; Malleret et al., 2021). This implies that P. vivax (Pv)RBP family proteins specifically target receptors unique to the reticulocyte membrane. Our previous studies on PvRBP1 of the P. vivax strain Belem (GenBank AAA29743.3) identified eleven high-affinity reticulocyte binding peptides (HABPs) corresponding to residues 158-653 of PvRBP1a in the P. vivax Salvador I strain (GenBank AAS85749.1). Among these, HABP 3742 (KLLGEEISEVSHLYV) and HABP 3459 (KEILDKMAKKVHYLK) exhibited dissociation constants (Kd) of 131 nM and 155 nM, respectively (Urquiza et al., 2002). Additionally, an extracellular portion of PvRBP1a, residues 157-650, binds strongly (~50%) to reticulocytes and moderately (~20%) to erythrocytes (Ntumngia et al., 2018). The identity of PvRBP1a₁₅₇₋₆₅₀ binding-receptors within the reticulocyte membrane has been unclear. Therefore, this study evaluated the erythroleukemic cell line JK-1 (Okuno et al., n.d) and the Bristol Erythroid Line Adult (BEL-A) (Trakarnsanga et al., 2017) as surrogates for reticulocytes, examining their susceptibility to P. vivax invasion. A comparison of the cell lines' membrane proteomes revealed similarities with those of reticulocytes, and dissimilarities with erythrocyte membrane proteomes, thereby identifying potential P. vivax receptors. Furthermore, TurboID proximity labelling implied specific interactions of PvRBP1a₁₅₈₋₆₅₀ with prohibitin-2 (PHB2), TfR1, and basigin (BSG). These interactions were confirmed by ELISA, highlighting key molecular determinants of P. vivax's reticulocyte tropism.

2 Materials and methods

2.1 Ethics statement

The study was conducted in accordance with the Declaration of Helsinki. Use of anonymized discarded blood from therapeutic phlebotomy was approved by the Institutional Review Board of City of Hope, Duarte, California, USA, as exempt category 4, under

10.3389/fcimb.2025.1671048 Molina-Franky et al.

45CFR46.104 (d). Blood samples from malaria patients were obtained under informed consent with the approval of the Bioethics central committee of the Universidad de Córdoba, Monteria, Colombia, and imported into the United States under CDC permit No.: 20210830-3188A0.

2.2 Collection, processing, and enrichment of P. vivax parasites from blood samples

P. vivax infected blood samples were collected from malaria patients in Tierralta-Córdoba, Colombia, into 5-mL sodium citrate tubes. After transportation to Bogotá, RBCs were enriched by centrifugation, mixed with an equal volume of Glycerolyte 57, cryopreserved, shipped to the U.S. lab, thawed using the NaCl method (Blomqvist, 2008), and resuspended in 3 mL of Iscove's Modified Dulbecco's Medium (IMDM). These RBCs were then enriched from 0.2% to 4.0% parasitemia by concentrating P. vivaxinfected reticulocytes through a KCl-Percoll gradient (Rangel et al., 2018). Enrichment was evaluated by microscopy with Giemsa staining (Figure 1A).

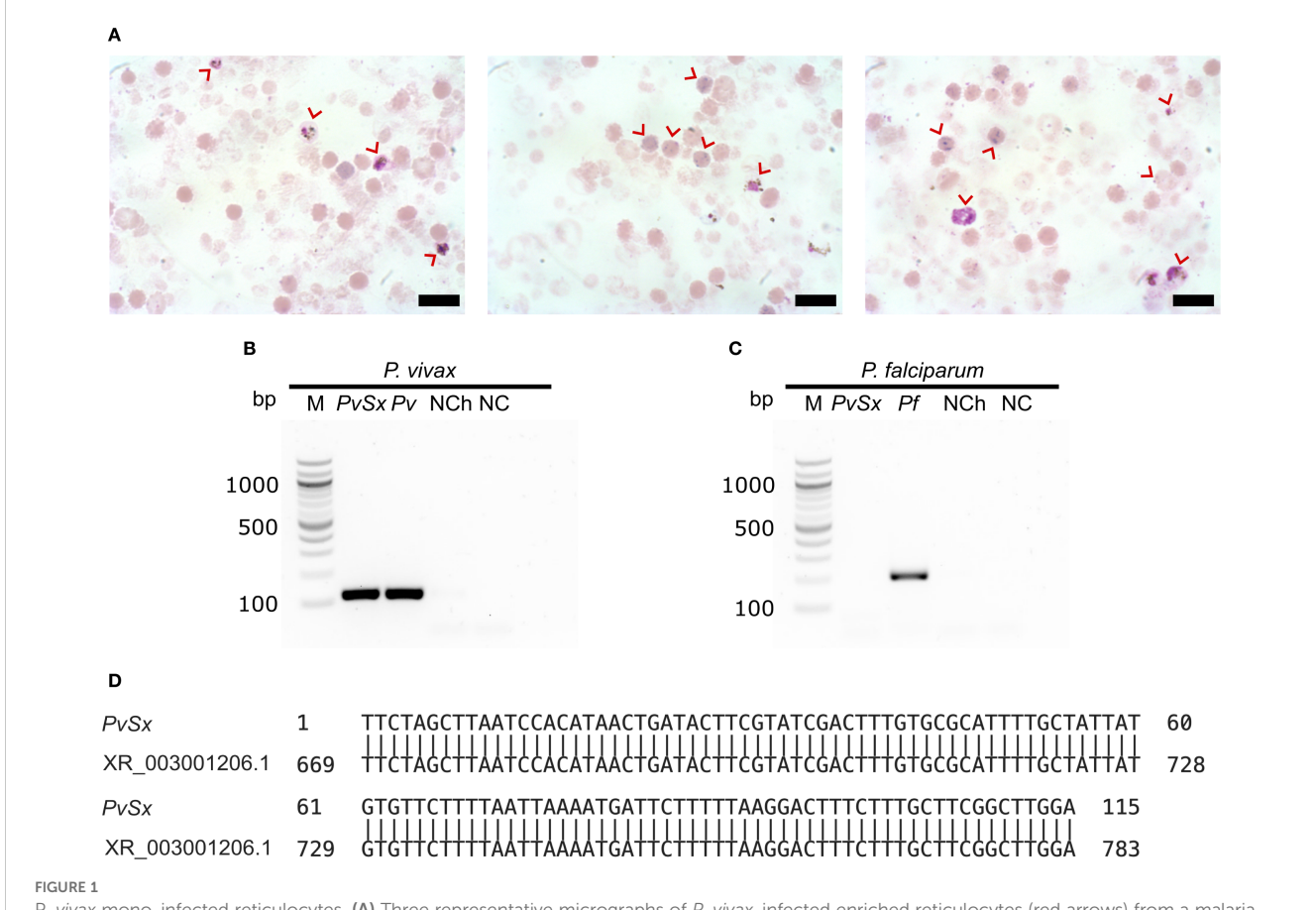
2.3 Identification of the Plasmodium species

Genomic DNA was extracted from infected cells, and nested PCR was performed using this DNA to identify the Plasmodium species. Genus- and species-specific primers targeting the parasite's 18S ribosomal small subunit RNA were used as previously described (Snounou et al., 1993) (see Supplementary Data).

2.4 P. vivax entry into BEL-A and JK-1 cells

JK-1 cells were obtained from the Deutsche Sammlung von Mikroorganismen und Zellkulturen GmbH (DSMZ) in Braunschweig, Germany, and BEL-A cells were from Prof. Dr. Jan Frayne of the University of Bristol, under contract by the NHS Blood and Transplant of the UK, see acknowledgement for details.

The enriched P. vivax mono-infected RBC sample (~40 µL) was divided into two equal aliquots, one for co-incubation with BEL-A cells and the other with JK-1 cells. Each cell line (1.5x105 cells) was cultured in 500 µL of medium, for BEL-A in StemSpan serum-free expansion



P. vivax mono-infected reticulocytes. (A) Three representative micrographs of P. vivax-infected enriched reticulocytes (red arrows) from a malaria patient. Scale bars are 3 µm. (B, C) Species-specific nested PCR for the small subunit 18S ribosomal RNA. Lane M, 100 bp marker; Lane PvSx, sample used in the infection of erythroid cells; Lanes Pv and Pf belong to the positive controls for each species; lane NCh, negative control using genomic DNA from a healthy human; lane NC, negative control using water instead of genomic DNA. (B) P. vivax (~120 bp amplicon). (C) P. falciparum (~205 bp amplicon). (D) DNA sequence alignment of the positive PvSx amplicon with the corresponding gene segment of the P. vivax Salvador-1 reference strain (GenBank No. XR_003001206.1) (Carlton et al., 2008), showing 100% identity

medium (SFEM, StemCell Technologies), containing 25% human serum (Type AB, Sigma-Aldrich), 50 ng/mL stem cell factor (SCF), 3 U/mL erythropoietin (EPO), 1 μ M dexamethasone, 1 μ g/mL doxycycline, 1 μ g/mL chemically defined lipid concentrate (CDLC), and 100 μ M hypoxanthine; and JK-1 in IMDM supplemented with GlutaMAX, with the same components, except for SCF, EPO, dexamethasone, and doxycycline. Both cultures were incubated at 37 °C with 5% CO2 and 5% O2. Fresh medium and 2×105 erythroid cells were added every two days, and cultures were evaluated by immunofluorescence assay (IFA) every 24 hours for 6 days (see Supplementary Data).

2.5 Quantitative comparison of membrane proteomes by (DIA) - LC-MS/MS

Reticulocytes, erythrocytes, JK-1 and BEL-A cells were collected, cytoplasmic content was removed by osmolytic lysis, and membrane proteins of the remaining ghosts were extracted. From each sample, 23 µg of proteins were processed for proteomics using S-Trap columns (ProtiFi) according to the manufacturer instructions (Matulis, 2016; HaileMariam et al., 2018). The resulting trypsin/LysC-digested peptides were analyzed by LC-MS/MS in data-independent acquisition (DIA) mode, as detailed in the Supplementary Data.

To enrich the plasma membrane proteins from the data set, proteins were filtered based on at least one of the following annotations from the UniProt subcellular localization database: "Cell membrane", "Apical cell membrane", "Basolateral cell membrane", "Peripheral membrane protein" and "Plasma membrane", and the Gene Ontology (GO) annotation term: "plasma membrane". The topology of the membrane proteins abundant in reticulocytes compared to erythrocytes was evaluated using several predictors. Protein sequences were analyzed with Protter for overall visualization of proteoforms (Omasits et al., 2014), TMHMM 2.0 for transmembrane region prediction (Hallgren et al., 2022), SignalP 6.0 for signal peptide identification (Teufel et al., 2022), and PredGPI for GPI anchor site prediction (Pierleoni et al., 2008).

2.6 PvRBP1A₁₅₈₋₆₅₀ proximity labeling for the identification of likely receptor candidates

2.6.1 Cloning, expression, purification, and activity of TurbolD fusion proteins

The DNA sequence encoding PvRBP1a₁₅₈₋₆₅₀ (GenBank AAS85749.1) was derived from the *P. vivax* Salvador I reference strain (txid126793). This sequence was fused to an acidic linker (L), GDEVDEDEG, to improve solubility, and the TurboID protein (TID) (Branon et al., 2018), followed by a C-terminal 6xHis tag for purification, resulting in the PvRBP1a₁₅₈₋₆₅₀LTID fusion protein. An equivalent gene encoding L with TurboID alone (LTID) was designed as a negative control. Both gene constructs were obtained as customized synthetic genes, optimized for expression in *E. coli*, and cloned into a pET-28a(+) expression vector between its NcoI and XhoI

sites. The constructs were expressed in soluble form in *E. coli* BL21 cells and purified by affinity chromatography, as detailed in the Supplementary Data. Protein purity and expression were verified by polyacrylamide gel electrophoresis. The biotinylation activity of both recombinant TurboID fusion proteins was confirmed by evaluating their autobiotinylation activity through incubation in the presence or absence of biotinylation reaction buffer Brxn (20 mM Tris-HCl, 500 µM biotin, 2.5 mM ATP, pH 7.5) at 37 °C for 15 minutes, quenching on ice and Western blot analysis with streptavidin-IRDye 800CW conjugate (1:1,000) and an Odyssey DLx imaging system (LICORbio).

2.6.2 PvRBP1a₁₅₈₋₆₅₀LTID proximity labeling

To evaluate PvRBP1a₁₅₈₋₆₅₀LTID's interaction with JK-1, BEL-A, reticulocytes, and erythrocytes, proximity labeling assays were performed in duplicate, and repeated up to three times. Cells were washed twice with PBS supplemented with 2% human serum (HS 2%) and incubated with either PvRBP1a₁₅₈₋₆₅₀LTID or LTID (negative control) for 3 hours at room temperature with constant mild agitation at 10 rpm. Following incubation, cells were washed three times with HS 2% to remove unbound proteins, then incubated with Brxn for 15 minutes at 37°C. The reaction was stopped by cooling on ice for 5 minutes, and the samples were washed with cold HS 2% before labeling with Alexa Fluor 488conjugated streptavidin (10 µg/mL, Invitrogen) for 1 hour at room temperature. Biotinylation was quantified by cytometry, acquiring 100,000 events per sample on a FACSAria Fusion (BD). Data were analyzed with FlowJo v10.8.1 (Ashland et al., 2023), calculating the percentage of biotinylated cells relative to total cells. LTID-treated and unlabeled cells served as negative controls.

2.6.3 The biochemical nature of $PvRBP1a_{158-650}$ receptors

JK-1 and BEL-A cells were treated with trypsin (1 mg/mL, Sigma-Aldrich), chymotrypsin (1 mg/mL, Sigma-Aldrich), or neuraminidase (50 mU, Roche) for 1 hour. After enzymatic treatment, proteolytic enzymes were inactivated with soy trypsin inhibitor (0.5 mg/mL, Sigma-Gibco) (Deans et al., 2007). Proximity labeling assays were then performed as described above, using $PvRBP1a_{158-650}LTID$ or LTID (3 μM).

2.6.4 Affinity enrichment and LC-MS identification of PvRBP1a₁₅₈₋₆₅₀ proximity-labeled receptor candidates

JK-1 cells were incubated with either PvRBP1a $_{158-650}$ LTID or LTID (negative control), each at 3 μ M for 3 hours. After incubation, cells were washed three times with HS 2%, then incubated with 100 μ L of Brxn for 15 minutes at 37°C. The reaction was stopped as described above, and cells were resuspended in 500 μ L of IP-MS lysis buffer (MS-compatible Magnetic IP kit, streptavidin, Pierce, Thermo Scientific), incubated on ice for 30 minutes with intermittent vortexing every 5 minutes. After centrifugation, the lysate's supernatant was collected and combined with Streptavidin magnetic beads (50 μ L, Thermo Scientific), incubated for 1 hour at 21°C, and then overnight at 4°C, to enrich biotinylated membrane proteins. The beads were washed, and

biotinylated proteins were eluted sequentially with 100 μL of 50 mM biotin, 100 μL of elution buffer, and 100 μL of 5% SDS at 95°C.

The eluted proteins were reduced, alkylated, and processed for proteomics using S-Trap spin columns (ProtiFi) according to the manufacturer's instructions (Matulis, 2016; HaileMariam et al., 2018). The resulting trypsin/LysC digested peptides were analyzed by LC-MS in data-dependent acquisition mode. Data analysis was performed using FragPipe v22.0 (Yu et al., 2021). Candidate receptor proteins for PvRBP1a₁₅₈₋₆₅₀ were selected based on the presence of extracellular regions that are favorable for ligand interaction, evaluated using UniProt GO annotations and the TMHMM 2.0 predictor (Hallgren et al., 2022). Receptor candidates in the PvRBP1a₁₅₈₋₆₅₀LTID sample that were detected in both duplicates and of significantly higher abundance (≥ 2 fold) compared to the negative control (LTID) were also considered. Subsequently, a parallel reaction monitoring (PRM) method was applied to validate and quantify the peptides of interest (as detailed in the Supplementary Data).

2.6.5 Binding affinities of PvRBP1a₁₅₈₋₆₅₀ to select receptor candidates by ELISA

The recombinant extracellular protein domains of receptor candidates TfR1 (Cys89-Phe760, SinoBiological), BSG (Met1-His205, SinoBiological), and full-length PHB2 (Origene) were used to evaluate the interaction between the PvRBP1a₁₅₈₋₆₅₀ and its binding membrane proteins (Supplementary Figure S1). Maxisorp plates were coated in triplicates with 5 µg/mL of each protein for 2 hours at room temperature and blocked with SuperBlock Buffer (Thermo Scientific). Serial dilutions of PvRBP1a₁₅₈₋₆₅₀LTID and LTID were prepared in blocking solution, ranging from 48,000 pM to 187.5 pM (1:2 dilution) and 4,000 pM to 1.28 pM (1:5 dilution), and incubated for 16 hours at 4°C. Bound PvRBP1a₁₅₈₋₆₅₀LTID and LTID were detected with a TurboID-specific polyclonal rabbit antibody (anti-BirA mutated/ TurboID, Agrisera, 1:10,000). After five washes with PBST, 100 µL of 3,3',5,5',-Tetramethylbenzidine (TMB) substrate was added, and the reaction was stopped with 50 µL of 1 M phosphoric acid. Absorbance was measured at 450 nm. Dissociation constants (Kd) were determined using GraphPad Prism v10.3.1 with non-linear regression and a one-site binding saturation model.

3 Results

3.1 *P. vivax* can invade the erythroid cell lines BEL-A and JK-1

Cultured BEL-A and JK-1 cells were successfully invaded by *P. vivax* from a validated mono-infected malaria patient's blood sample. The experiment required forgoing enrichment of the RBCs to 4.0% parasitemia (Figures 1A–D). Parasite invasion was confirmed by immunofluorescence microscopy, detecting the intracellular presence of *P. vivax* lactate dehydrogenase (PvLDH), which all blood stages of the parasite are known to express (Cao et al., 2024). PvLDH was detected in the positive control of infected

reticulocytes, and in BEL-A and JK-1 cells, incubated with infected reticulocytes (Figure 2, FITC). The PvLDH signal was absent from non-infected control cells. Moreover, the presence of hemozoin (Hz) pigment, characteristic for hemoglobin consumption by Plasmodia within infected RBCs (Pandey and Tekwani, 1996), was observed (Figure 2, bright field, and merge). The dark Hz pigment was visible inside the parasite-infected nucleated erythroid cells as well as in infected reticulocytes that originated from the donor. Hz is an insoluble, crystallized digestion product of heme derived from the digestion of hemoglobin by malaria parasites, containing heme-derived \(\beta \)-hematin, which neutralizes the toxicity of free heme released after parasite invasion through a digestive process that involves the digestive vacuole structure (Coronado et al., 2014). On days 3 to 6 post-infection, no parasite-infected erythroid cells were observed, and cell mortality had substantially increased. Therefore, the experiment was stopped on day 6.

3.2 Overlapping membrane proteomes reveal potential *P. vivax* invasion receptors

Because *P. vivax* was able to invade the erythroid BEL-A and JK-1 cells, their membranes must contain the same essential receptor molecules as reticulocytes that enable parasite invasion. Furthermore, the membranes of mature erythrocytes are expected to lack these receptors or to express them only at insufficient abundances. Consequently, a quantitative comparison of the membrane proteome of these cells with those of human reticulocytes and erythrocytes identified potential receptors for *P. vivax* merozoite ligands that are most likely responsible for its reticulocyte-restricted invasion.

Stringent isolation procedures were necessary to obtain membrane proteins of pure reticulocytes. The isolated reticulocytes (CD71⁺, CD45⁻) used in this proteomic comparison had a purity of 98.4% (Supplementary Figure S2). Expression of CD71 is diminished during maturation into fully functional erythrocytes (Malleret et al., 2015b). Simultaneous determination of CD45 negativity was necessary, as CD45⁺ leukocytes also express CD71, to ensure purity of the isolated reticulocytes.

The BEL-A and JK-1 cells used in the membrane proteomic comparisons were harvested from *in vitro* cultures and exhibited distinct nucleated erythroid maturation stages, including proerythroblasts, basophilic erythroblasts, polychromatic erythroblasts, and orthochromatic erythroblasts (Supplementary Figure S3), with slight dominance of the basophilic and polychromatic stages.

In total, 2,100 proteins were identified in BEL-A cells and 2,178 in JK-1 cells. The number of proteins was lower in reticulocytes (1,234) and in erythrocytes (1,347). After filtering this data for membrane proteins (see Supplementary Data, Supplementary Figure S4), 1,530 and 1,595 such proteins were obtained from BEL-A and JK-1 cell ghosts, respectively, while 846 and 974 proteins were identified for reticulocyte and erythrocyte ghosts.

Changes in membrane protein abundance were assessed by comparing erythroid cell lines and reticulocytes to mature

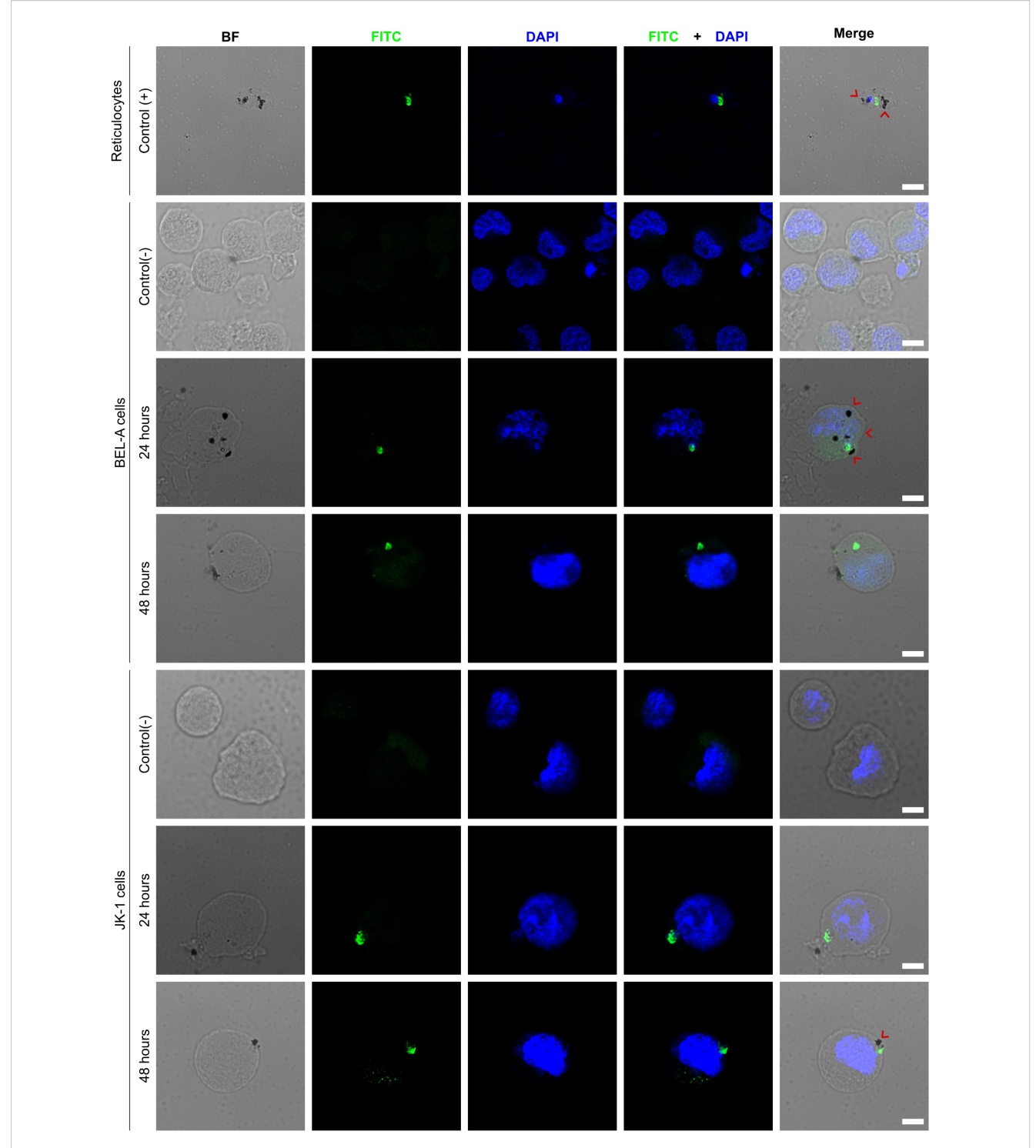
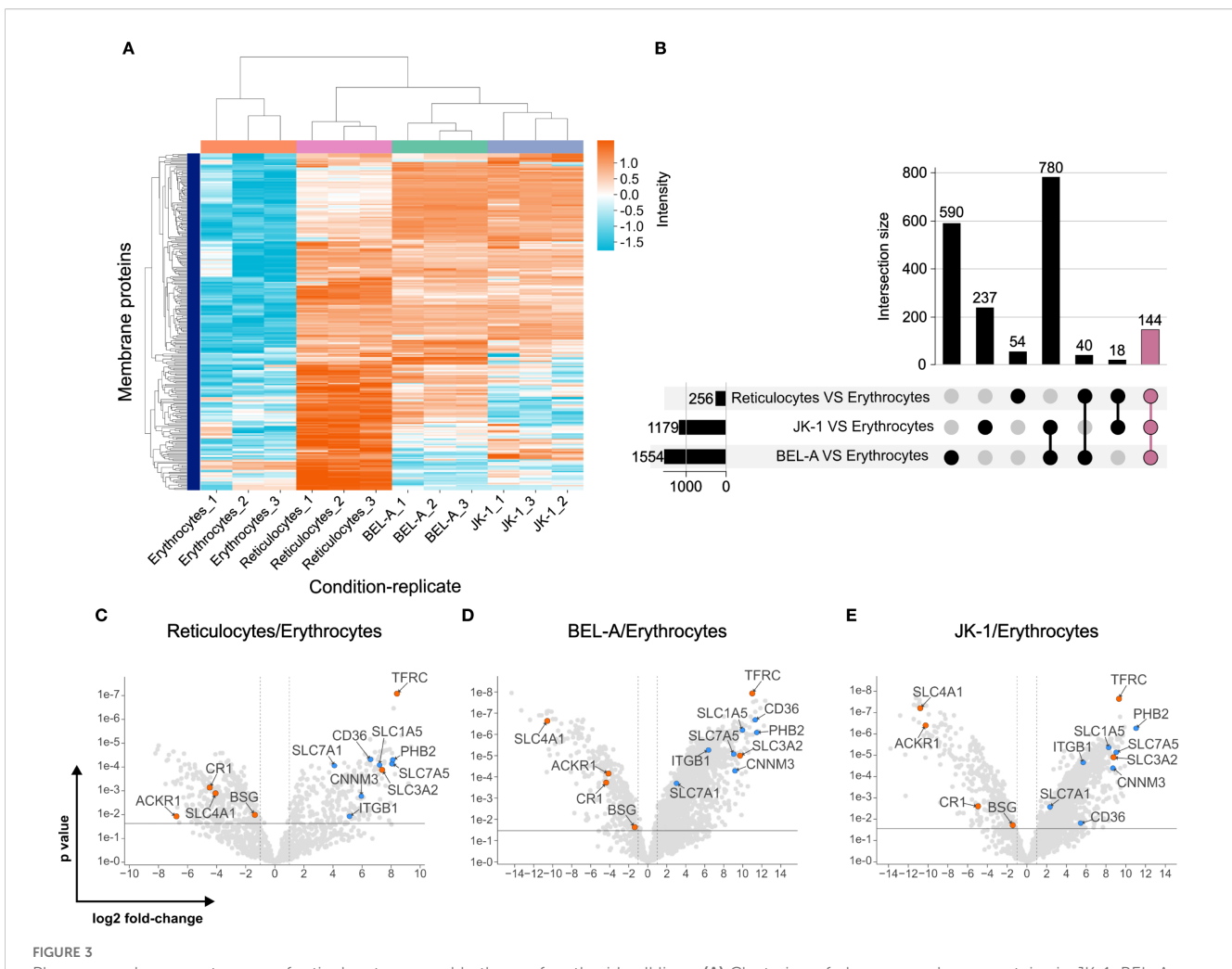


FIGURE 2
P. vivax invades BEL-A and JK-1 cells. The micrographs show P. vivax-infected reticulocytes as the positive Control (+); infected BEL-A and JK-1 cells at 24 and 48 h, and their non-infected negative Control (-); P. vivax lactate dehydrogenase (FITC green); DNA (DAPI blue); hemozoin crystals (black dots marked with red arrows); BF (bright field); Scale bars are 5 µm.

erythrocytes. The protein abundancies of reticulocytes clustered better with those of BEL-A and JK-1 cells than with those of erythrocytes (Figure 3A). It was found that compared to erythrocytes 256 proteins were more abundant in reticulocytes, 1,179 in JK-1, and 1,554 in BEL-A. Of these, 144 identical proteins

were increased in reticulocytes, JK-1, and BEL-A. However, reticulocytes and JK-1 cells share 18 proteins that are less abundant in erythrocytes, while BEL-A and reticulocytes have 40 proteins in common, that are less abundant in erythrocytes. Only 54 membrane proteins with higher abundance than in erythrocytes



Plasma membrane proteomes of reticulocytes resemble those of erythroid cell lines. (A) Clustering of plasma membrane proteins in JK-1, BEL-A, reticulocytes, and erythrocytes, measured in triplicate. Log2 intensities. (B) Abundance of intersecting membrane proteins in reticulocytes, JK-1, and BEL-A cells compared to erythrocytes, represented in an UpSet plot (Lex et al., 2014). 144 proteins share higher abundance among cell lines and reticulocytes but are reduced in erythrocytes (mauve bar). (C-E) Putative receptors (blue) and characterized receptors (orange) for *P. vivax* merozoite invasion. Gene names are displayed instead of protein names for simplicity. The x-axis represents the log2 fold change, and the y-axis shows the P-value, indicating statistical significance.

were identified exclusively in reticulocytes, 237 in JK-1, and 590 in BEL-A cells (Figure 3B).

When comparing the membrane protein abundance in reticulocytes, cell lines, and erythrocytes, known *P. vivax* receptors such as TfR1 (CD71), CD98hc, ACKR1/DARC, BSG, CR1, and band 3 (SLC4A1) were identified. TfR1 and CD98hc, which are lost during reticulocyte maturation to erythrocytes, were significantly more abundant in reticulocytes and cell lines. In contrast, the other receptors showed higher levels in erythrocytes (Figures 3C–E).

In silico topological analysis of membrane proteins enriched in reticulocytes and erythroid cell lines identified several candidates — CD98lc (SLC7A5), high-affinity cationic amino acid transporter 1 (CAT-1, SLC7A1), neutral amino acid transporter B0 (ATB(0), SLC1A5), CD36, Integrin β -1 (ITGB1), prohibitin-2 (PHB2), and the metal transporter CNNM3 — as possessing sizable extracellular regions that are potentially accessible for interaction with *P. vivax* merozoite ligands (Supplementary Table S1, Supplementary Figure S5).

The significantly higher abundance of these proteins in reticulocytes, BEL-A, and JK-1 cells compared to erythrocytes (Figures 3C–E; Supplementary Table S1) highlights them as potential candidates for *P. vivax* merozoite protein receptors, which may explain the parasite's exclusivity for reticulocyte invasion.

3.3 Receptors for PvRBP1a₁₅₈₋₆₅₀LTID identified via proximity labeling

To identify potential receptors of the PvRBP1a₁₅₈₋₆₅₀LTID protein, the TurboID proximity labeling technique was used. This technique enables the biotinylation of proteins that come into close contact with the fused protein (within 10 nm), facilitating the identification of their interactions (Branon et al., 2018; Cho et al., 2020). Therefore, the fusion protein PvRBP1a₁₅₈₋₆₅₀LTID and the LTID control were obtained in soluble form, with PvRBP1a₁₅₈₋₆₅₀LTID having a molecular weight of ~94 kDa and LTID ~36 kDa

(Figure 4A). Both proteins exhibited enzymatic activity and self-biotinylation at 1, 2, and 3 μM (Figures 4B, C).

3.4 PvRBP1a₁₅₈₋₆₅₀LTID exhibits comparable binding to reticulocytes and erythroid cell lines via a proteinaceous receptor

Proximity biotinylation mediated by TurboID facilitated binding evaluation through the biotin-streptavidin interaction. The assays showed that PvRBP1a₁₅₈₋₆₅₀LTID binding is concentration-dependent (Figure 4D). Since the highest percentage of biotin labeling on the cell surface was obtained at 3 μM, this concentration was selected to analyze PvRBP1a₁₅₈₋₆₅₀LTID binding to enriched reticulocytes (87.5% purity) (Supplementary Figure S6), erythrocytes, and cell lines. The results showed that PvRBP1a₁₅₈₋₆₅₀ had 80% biotinylation on the surface of reticulocytes, 4.7% on erythrocytes, and 79.85% and 83.2% on the surface of JK-1 and BEL-A cells, respectively. A statistically significant difference was found between the cell lines and reticulocytes compared to erythrocytes (P ≤ 0.0001). However, no significant difference was observed between the cell lines and reticulocytes (Figures 4E, F). These data suggest that erythroid cell lines exhibit PvRBP1a₁₅₈₋₆₅₀ binding activity comparable to reticulocytes, indicating that they may express the receptor for this specific P. vivax ligand on their surface. Additionally, no labelling was detected with LTID, confirming the specificity of the PvRBP1a₁₅₈₋₆₅₀ receptor interaction.

Cell surface labelling with PvRBP1a₁₅₈₋₆₅₀LTID was sensitive to trypsin and chymotrypsin treatment but resistant to neuraminidase, which removes sialic acid from glycans that modify proteins in vertebrates (Figure 4G). Therefore, the cell surface receptor function for PvRBP1a₁₅₈₋₆₅₀ is proteinaceous and not dependent on sialic acid-terminated glycans.

3.5 Enrichment of PvRBP1a₁₅₈₋₆₅₀LTID biotinylated cell surface proteins, identifies TfR1 and prohibitin-2 as the likely reticulocyte-restricting receptors

PvRBP1a₁₅₈₋₆₅₀LTID biotinylated membrane proteins from erythroid cells were captured via streptavidin-affinity and subjected to proteomics analysis, revealing a total of 278 proteins, of which 12 were localized to the plasma membrane. However, the LTID control contained five of these proteins, leaving seven unique to enrichment after biotinylation with PvRBP1a₁₅₈₋₆₅₀LTID. Four of these membrane proteins do not possess extracellular regions, while TfR1, prohibitin-2, and BSG do. Such extracellular regions should be required to facilitate an interaction with *P. vivax* merozoite ligands (Figure 5A). Interaction of PvRBP1a₁₅₈₋₆₅₀ was successfully validated by targeted PRM LC-MS analysis for TfR1, BSG, and prohibitin-2 (Figure 5B). It clearly demonstrated that only PvRBP1a₁₅₈₋₆₅₀LTID biotinylated these three proteins, while LTID did not.

BSG is more abundant in erythrocytes than in reticulocytes and in the erythroid cell lines. In contrast, TfR1 and prohibitin-2 were significantly less abundant in erythrocytes (Figures 3C–E). In fact, TfR1 and prohibitin-2 were among the most abundant membrane proteins in reticulocytes and in the erythroid cell lines JK-1 and BEL-A. These findings suggest that PvRBP1a₁₅₈₋₆₅₀ likely facilitate the recognition and invasion of reticulocytes through interaction with TfR1 and prohibitin-2.

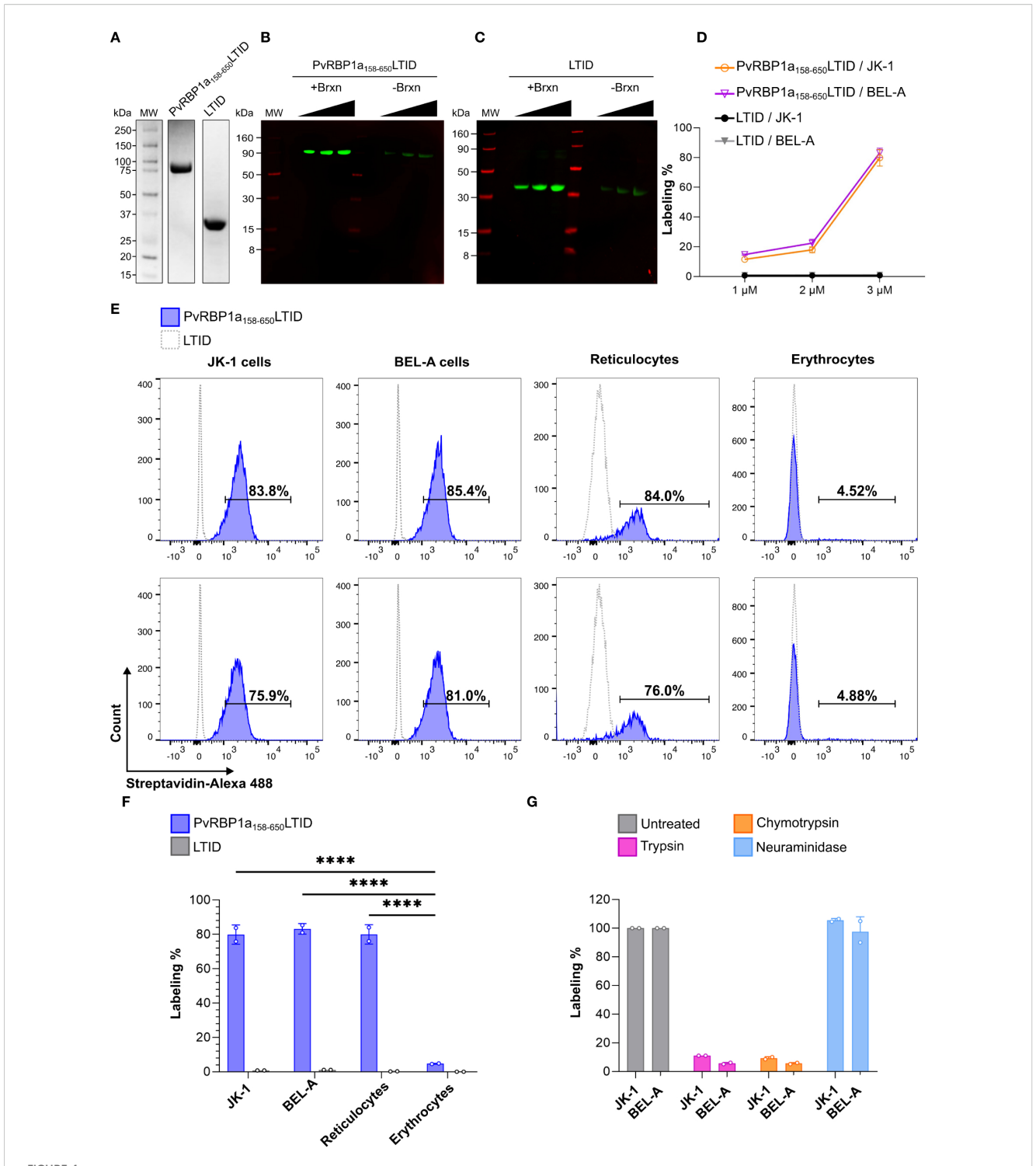
3.6 PvRBP1a₁₅₈₋₆₅₀LTID interacts with high-affinity binding to TfR1, BSG, and prohibitin-2

The titration curves fit well to a single-site binding saturation model. In contrast, the negative control LTID displayed a nonspecific binding pattern "unstable", corroborating the specificity of the interactions (Figure 6A). The Kd obtained from the ELISA titration indicated that PvRBP1a₁₅₈₋₆₅₀LTID had high affinity for TfR1 (Kd: 1.15 nM), followed by BSG (Kd: 2.16 nM) and prohibitin-2 (Kd: 2.77 nM) (Figure 6B).

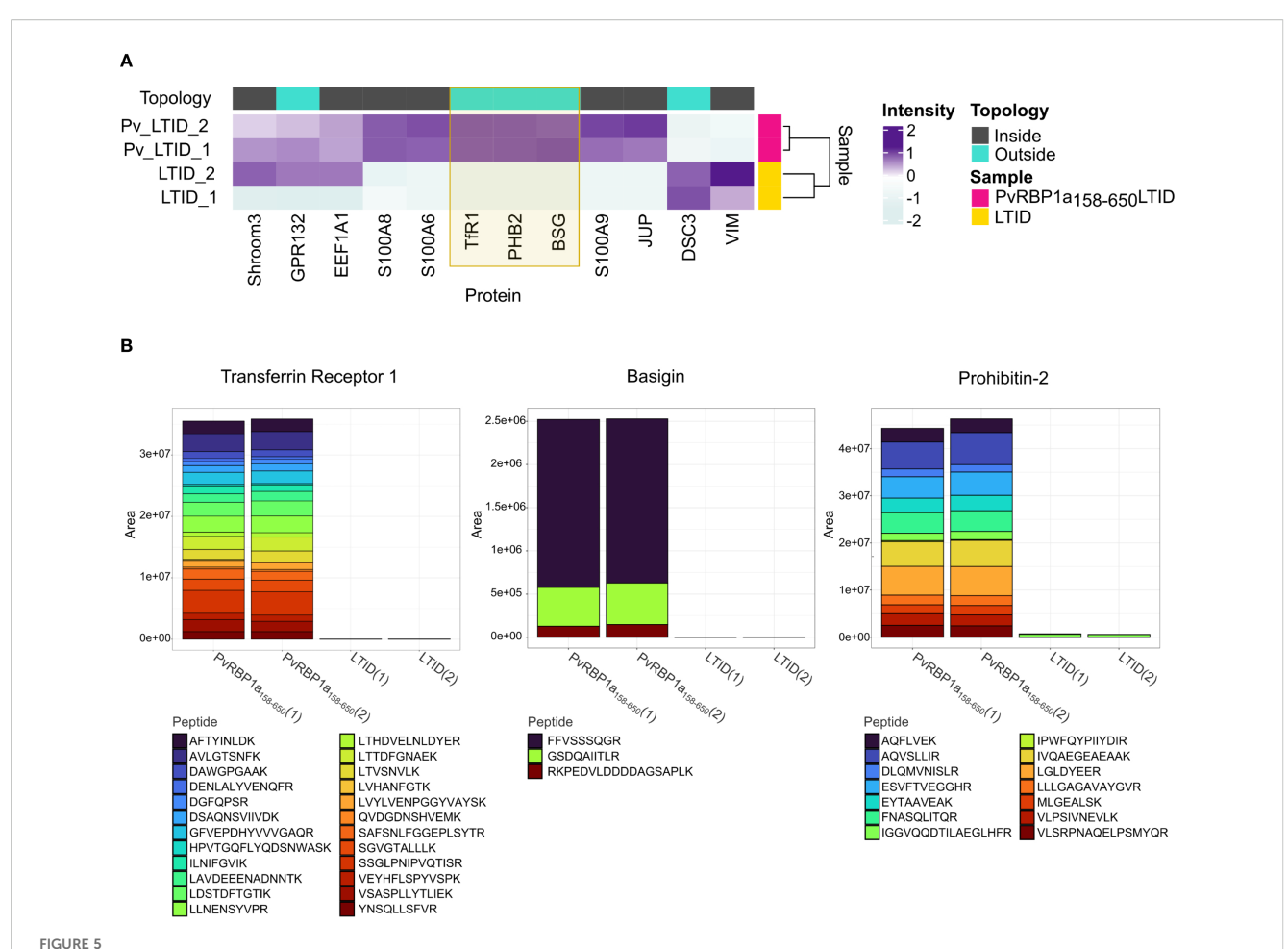
4 Discussion

This study demonstrates the utility of erythroid cell lines JK-1 and BEL-A as suitable surrogates for reticulocytes for studying the invasion process of the *P. vivax* malaria parasite. While these cell lines and their culture conditions did not support a continuous *P. vivax* culture *in vitro*, the formation of the Hz pigment and immuno detection of PvLDH strongly supported parasite invasion. In contrast to human reticulocytes, both erythroid cell lines are nucleated, which might permit them to initiate a cell-death program upon parasite invasion. Consistently, JK-1 cells were previously reported to support cell entry by both *P. vivax* and *P. falciparum* (Kanjee et al., 2017; Gruszczyk et al., 2018b), while BEL-A cells have so far only been studied with *P. falciparum* (Satchwell et al., 2019). This study is the first to report *P. vivax* invasion of BEL-A cells, confirming their susceptibility alongside JK-1 cells.

The quantitative membrane proteome comparison of reticulocytes and erythroid cell lines with erythrocytes revealed Prohibitin-2 (PHB2), TfR1 (CD71), the CD98 heavy chain (4F2hc, gene SLC3A2), the CD98 light chain (LAT-1, gene SLC7A5), ATB (0) (gene SLC1A5), CAT-1 (SLC7A1), CD36, Integrin β-1 (gene ITGB1), and Metal transporter CNNM3 to be of significantly increased abundance in those cell lines and reticulocytes. Whereas they are strongly decreased (practically absent) in fully matured erythrocytes. The increased abundance of TfR1 and CD98 in reticulocytes over erythrocytes is consistent with previous studies (Malleret et al., 2015b, 2021). However, genetic manipulation (Gruszczyk et al., 2018a) or antibody blockade (Malleret et al., 2021) of these proteins only partially reduced P. vivax invasion, suggesting the involvement of additional receptors. The heavy chain of CD98 (SLC3A2) was reported to be bound by P. vivax in immature RBCs via PvRBP2a (Malleret et al., 2021). Therefore,



Proximity labeling with PvRBP1a₁₅₈₋₆₅₀LTID in JK-1, BEL-A, reticulocytes, and erythrocytes. Recombinantly expressed soluble PvRBP1a₁₅₈₋₆₅₀LTID and LTID by **(A)** SDS PAGE **(B, C)** auto-biotinylation assay with increasing concentrations of each protein at 1, 2, and 3 μ M, detected with IRDye 800 Streptavidin (green bands), LICORbio molecular weight markers (MW, red bands); **(D)** biotin labeling of JK-1 (orange) and BEL-A (fuchsia) cells, in presence of PvRBP1a₁₅₈₋₆₅₀LTID or LTID (negative control, JK-1 - black, and BEL-A - gray) at 1, 2, and 3 μ M. **(E-G)** Flow cytometry **(E)** histograms of erythroid cells and human RBCs in presence of PvRBP1a₁₅₈₋₆₅₀LTID (blue) or LTID (grey), both at 3 μ M, demonstrating **(F)** significant degrees of cell surface labeling by PvRBP1a₁₅₈₋₆₅₀LTID in erythroid cells and reticulocytes compared to erythrocytes (****p \leq 0.0001). **(G)** Receptors to PvRBP1a₁₅₈₋₆₅₀ are sensitive to cell surface treatment with trypsin and chymotrypsin but resistant to neuraminidase (labeling % as normalized to untreated cells).



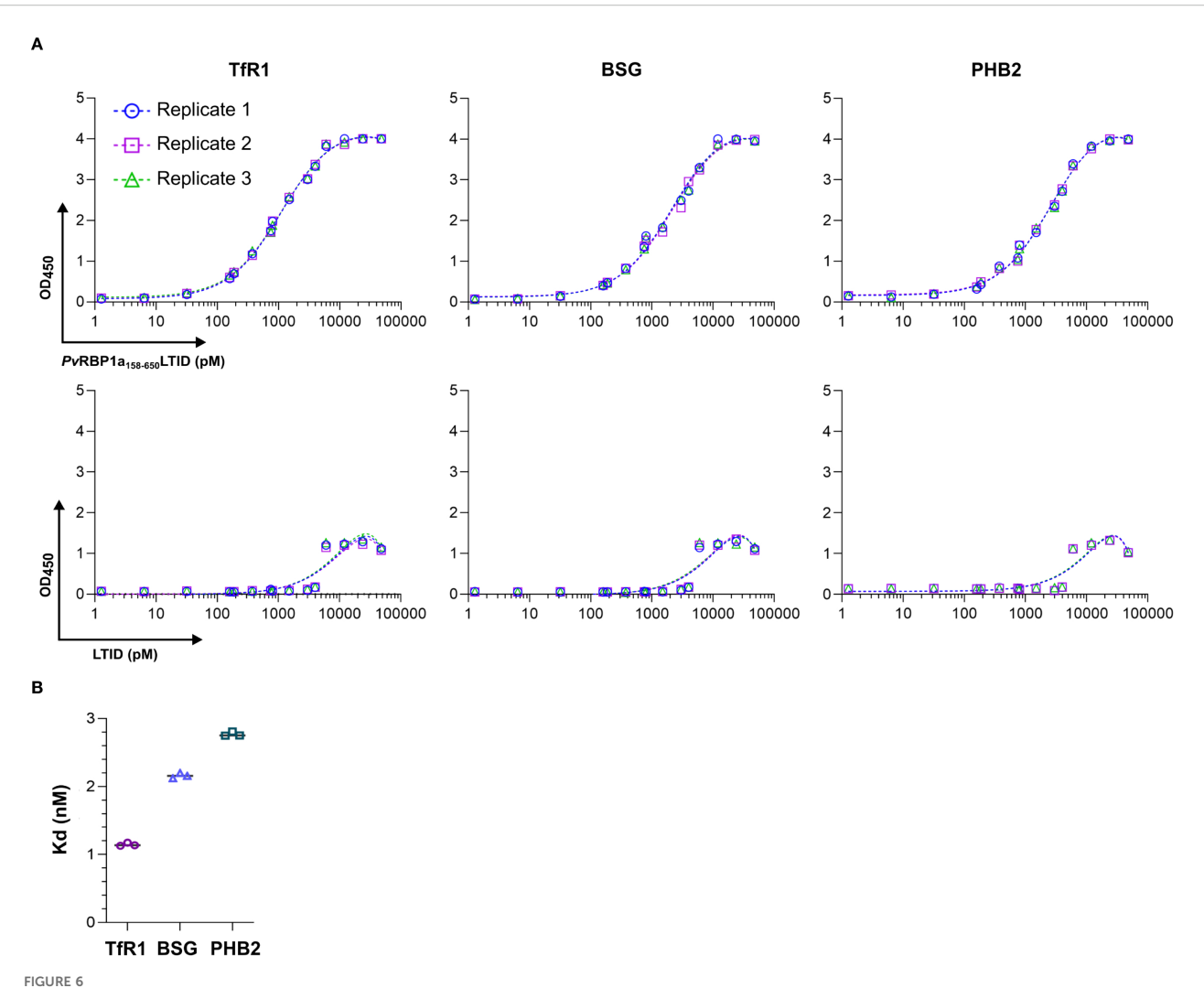
Proximity biotin-labeled TfR1 (CD71), Basigin, and Prohibitin-2, are identified as *P. vivax* receptor candidates after interaction of JK-1 cells with PvRBP1a₁₅₈₋₆₅₀LTID and validated by targeted LC-MS. (A) Heatmap of labeled plasma membrane protein intensities in the PvRBP1a₁₅₈₋₆₅₀LITD (fuchsia) and LTID (yellow) control samples, analyzed in duplicate by DDA LC-MS proteomics. Intensities are represented on a Z-score scale, where each value was transformed by the number of standard deviations (SD) from the mean. Topology categorizes proteins by their cellular localization: intracellular (Inside, dark gray) and those with extracellular domains (Outside, cyan). They include Shroom3, GPR132 – probable G-protein coupled receptor 132, EEF1A1 – Elongation factor 1-alpha 1, protein S100-A8, protein S100-A6, TfR1, PHB2 – prohibitin-2, BSG, protein S100-A9, JUP – junction plakoglobin, DSC3 – Desmocollin-3, and VIM – vimentin. (B) Validated interactions of transferrin receptor 1, basigin, and prohibitin-2 with PvRBP1a₁₅₈₋₆₅₀LITD, but not with LITD, during the TurboID procedure, followed by PRM LC-MS. (1) (2) – duplicates. Stacked bars are the sum of the LC-MS ion chromatographic peak areas of the trypsin digested peptides (colored boxes) of each protein, indicating the contribution of each peptide to the individual protein abundance.

other potential *P. vivax* receptor candidates with extracellular regions, namely Prohibitin-2, the CD98 light chain (LAT-1), ATB (0), CAT-1, CD36, Integrin β-1, and CNNM3 should be considered. These membrane proteins participate in various protein-protein interactions that facilitate the entry of microorganisms into host cells (Albritton et al., 1993; Yoshimoto et al., 1993; Smith et al., 1998; Tailor et al., 1999; Graham et al., 2003; Weigel-Kelley et al., 2003; Maginnis et al., 2006; Xiao et al., 2008; Feire et al., 2010; Nägele et al., 2011; Wintachai et al., 2012; Su et al., 2020; Olaya-Galán et al., 2021). Interestingly, LAT-1, that together with its heavy chain 4F2hc forms the heteromeric CD98 (Lee et al., 2019; Yan et al., 2019), plays a role in hepatitis C virus entry (Nguyen et al., 2018), raising the question of whether *P. vivax* may also interact with LAT-1.

Proximity labeling of erythroid cells with PvRBP1a $_{158-650}$ LTID was largely consistent with previous observations, in which $\sim 50\%$ of

reticulocytes binding and ~20% of erythrocytes bound to PvRBP1a₁₅₇₋₆₅₀ (Ntumngia et al., 2018). Furthermore, 20 of reticulocytes and only 1% of erythrocytes bound to PvRBP1a351-599 (Han et al., 2016), while 31.5% of reticulocytes were reported to bind to PvRBP1a30-778 (Gupta et al., 2017). Additionally, the trypsin and chymotrypsin sensitivity of these recombinant protein (Han et al., 2016; Gupta et al., 2017; Ntumngia et al., 2018), as well as the PvRBP1a157-653 HAPBs (Urquiza et al., 2002) align with our results.

 $PvRBP1a_{158-650}$ was found to interact with Prohibitin-2, TfR1, and BSG. Prohibitin-2 and TfR1 are more abundant in reticulocyte membranes and cell lines compared to erythrocytes, while BSG is more abundant in erythrocytes. These findings suggest that $PvRBP1a_{158-650}$ may facilitate reticulocyte recognition and invasion through interaction with Prohibitin-2 and TfR1. Additionally, interaction with BSG may contribute to binding activity to erythrocytes, but not their restricted invasion, consistent with



PVRBP1a₁₅₈₋₆₅₀ binds to TfR1, BSG, and PHB2 at nanomolar affinities. **(A)** Titration ELISAs of protein-protein interactions between soluble ligand PVRBP1a₁₅₈₋₆₅₀LTID, control LTID, and the immobilized receptor candidates TfR1, BSG, and PHB2. OD450 absorbance values represent the binding of a TurbolD-specific HRP-labeled antibody for the biotin-free quantification of ligand and control in triplicate, fitted by a single-site binding model; **(B)** average dissociation constants (kd) summarized as determined from the fitted titration curves above.

previous studies on PvRBP1a binding (Urquiza et al., 2002; Han et al., 2016; Gupta et al., 2017; Ntumngia et al., 2018).

This study demonstrated strong binding of PvRBP1a₁₅₈₋₆₅₀ with the 89-760 domain of TfR1, contrasting with prior work that did not detect this interaction, possibly due to the crucial role of TfR1's 89-120 region, not included in the previous protein construct (Gruszczyk et al., 2018b). TfR1 is a known receptor for PvRBP2b (Gruszczyk et al., 2018a), as well as for various New World arenaviruses (Radoshitzky et al., 2007, 2008).

Prohibitin-2 has been implicated in facilitating the entry of diverse viruses, including enteroviruses, coronaviruses, HIV-1, and flaviviruses such as dengue (Cornillez-Ty et al., 2009; Emerson et al., 2010; Kuadkitkan et al., 2010; Su et al., 2020). Although traditionally characterized as a protein of the inner mitochondrial membrane and nucleus, subsequent studies have demonstrated its presence at the plasma membrane, notably in CHME-5 microglial cells and RMS cells (Wintachai et al., 2012; Fu et al., 2013). Its established

function as a receptor or co-receptor for several pathogens further supports the notion that prohibitin-2 can localize to the cell surface, where it may contribute to pathogen attachment and entry.

BSG, a known receptor for *P. falciparum* RH5 (Crosnier et al., 2011; Chen et al., 2014), a member of the PfRH family homologous to the PvRBP proteins of *P. vivax* (Rayner et al., 2000; Triglia et al., 2001), also serves as a receptor for *P. vivax* TRAg38 (Rathore et al., 2017). In addition, PvRBP1 is the orthologue of *P. falciparum* normocyte binding protein 1 (PfNBP1) (Rayner et al., 2001), and PvRBP1a (N352–K598) shares sequence homology with PfRH4 (N328–D588) (Gaur et al., 2007), although these proteins engage different host receptors. Interestingly, PvRBP2a, which binds TfR1 in *P. vivax*, displays a structural scaffold similar to PfRH5 of *P. falciparum* (Gruszczyk et al., 2016), highlighting that orthologous and homologous relationships can provide an evolutionary framework to interpret invasion mechanisms even when receptor usage differs. Such cross-species comparisons are a common

approach in malaria research (Tebben et al., 2022) and contextualize our findings on PvRBP1a interactions.

This research demonstrated the binding versatile of PvRBP1a₁₅₈₋₆₅₀, which interacts with three different membrane proteins. In biological systems, ligands often bind multiple receptors, as seen with *Plasmodium* interactions; PvTRAg38 binds both BSG and band 3 (Alam et al., 2016, p. 3; Rathore et al., 2017), and PfEMP1binds to several receptors (Yipp et al., 2000; Vogt et al., 2003; Vigan-Womas et al., 2012; Esser et al., 2014; Kessler et al., 2017).

This study demonstrates that the BEL-A and JK-1 cells are suitable models for studying *P. vivax* receptor-ligand interactions, providing viable alternatives to reticulocytes. The similarity in the abundance of potential receptor candidates between cell lines and reticulocytes, and their dissimilarity with erythrocytes, validates the use of JK-1 and BEL-A cell lines as surrogate models for the study of *P. vivax* merozoite ligand-receptor interactions, and suggests the existence of other potential *P. vivax* receptors. prohibitin-2 and TfR1 may contribute to a redundant reticulocyte-restricted invasion pathway because they exhibit high binding affinities to PvRBP1a₁₅₈₋₆₅₀. These findings lay the foundation for the comprehensive study of all *P. vivax* invasion mechanisms and for the development of targeted therapies against malaria.

Data availability statement

LC-MS DIA data was deposited to the MassIVE repository at the Center for Computational Mass Spectrometry, University of California, San Diego under Dataset Identifier: MSV000093438 (https://doi.org/doi:10.25345/C5W669K65). The DDA and PRM LC-MS data sets are available under MSV000096045 (https://doi.org/doi:10.25345/C5Q52FR0R).

Ethics statement

The studies involving humans were approved by Bioethics central committee of the Universidad de Córdoba, Monteria, Colombia. Import permit by the United States CDC: 20210830-3188A0. The studies were conducted in accordance with the local legislation and institutional requirements. The participants provided their written informed consent to participate in this study.

Author contributions

JM-F: Conceptualization, Data curation, Formal analysis, Investigation, Methodology, Software, Validation, Visualization, Writing – original draft, Writing – review & editing. DR: Methodology, Software, Writing – review & editing. MA-S: Methodology, Writing – review & editing. MP: Conceptualization, Data curation, Investigation, Supervision, Writing – review & editing. MK: Conceptualization, Formal analysis, Funding acquisition, Methodology, Project administration, Resources, Supervision, Writing – review & editing, Data curation, Investigation, Validation.

Funding

The author(s) declare financial support was received for the research and/or publication of this article. This study was funded in parts by the Memorial Hermann Foundation with a grant to MK in support of MK, DR, and JMF. The authors declare that no financial support was received for the authorship or publication of this article.

Acknowledgments

The authors are grateful to NHS Blood and Transplant, especially Professor Jan Frayne, for providing the BEL-A cell line. "BEL-A cell lines were created by Professor Jan Frayne, Professor David Anstee and Dr Kongtana Trakarnsanga with funding from the Wellcome Trust (grant numbers 087430/Z/08 and 102610), NHS Blood and Transplant and Department of Health (England)". Furthermore, they wish to extend their gratitude to the "Grupo de Investigaciones Microbiológicas y Biomédicas de Córdoba – GIMBIC" from the Universidad de Córdoba, Colombia, for providing the P. vivax samples. The authors dedicate this study to Professor Manuel Elkin Patarroyo (1946-2025), in loving memory.

Conflict of interest

The authors declare that the research was conducted in the absence of any commercial or financial relationships that could be construed as a potential conflict of interest.

Generative AI statement

The author(s) declare that no Generative AI was used in the creation of this manuscript.

Any alternative text (alt text) provided alongside figures in this article has been generated by Frontiers with the support of artificial intelligence and reasonable efforts have been made to ensure accuracy, including review by the authors wherever possible. If you identify any issues, please contact us.

Publisher's note

All claims expressed in this article are solely those of the authors and do not necessarily represent those of their affiliated organizations, or those of the publisher, the editors and the reviewers. Any product that may be evaluated in this article, or claim that may be made by its manufacturer, is not guaranteed or endorsed by the publisher.

Supplementary material

The Supplementary Material for this article can be found online at: https://www.frontiersin.org/articles/10.3389/fcimb.2025. 1671048/full#supplementary-material

References

Alam, M. S., Rathore, S., Tyagi, R. K., and Sharma, Y. D. (2016). Host-parasite interaction: multiple sites in the *Plasmodium vivax* tryptophan-rich antigen PvTRAg38 interact with the erythrocyte receptor band 3. *FEBS Lett.* 590, 232–241. doi: 10.1002/1873-3468.12053

Albritton, L. M., Kim, J. W., Tseng, L., and Cunningham, J. M. (1993). Envelope-binding domain in the cationic amino acid transporter determines the host range of ecotropic murine retroviruses. *J. Virol.* 67, 2091–2096. doi: 10.1128/jvi.67.4.2091-2096.1993

Ashland, O. R., Becton,, and Dickinson and Company (2023). FlowJoTM Software (for Windows) Version 10.8.1

Blomqvist, K. (2008). Thawing of glycerolyte-frozen parasites with NaCl. Methods Malaria Res. 15.

Branon, T. C., Bosch, J. A., Sanchez, A. D., Udeshi, N. D., Svinkina, T., Carr, S. A., et al. (2018). Efficient proximity labeling in living cells and organisms with TurboID. *Nat. Biotechnol.* 36, 880–887. doi: 10.1038/nbt.4201

Cao, P., Kho, S., Grigg, M. J., Barber, B. E., Piera, K. A., William, T., et al. (2024). Characterisation of *Plasmodium vivax* lactate dehydrogenase dynamics in *Plasmodium vivax* infections. *Commun. Biol.* 7, 355. doi: 10.1038/s42003-024-05956-6

Carlton, J. M., Adams, J. H., Silva, J. C., Bidwell, S. L., Lorenzi, H., Caler, E., et al. (2008). Comparative genomics of the neglected human malaria parasite *Plasmodium vivax*. *Nature* 455, 757–763. doi: 10.1038/nature07327

Chen, L., Xu, Y., Healer, J., Thompson, J. K., Smith, B. J., Lawrence, M. C., et al. (2014). Crystal structure of PfRh5, an essential *Plasmodium falciparum* ligand for invasion of human erythrocytes. *eLife* 3, e04187. doi: 10.7554/eLife.04187

Cho, K. F., Branon, T. C., Udeshi, N. D., Myers, S. A., Carr, S. A., and Ting, A. Y. (2020). Proximity labeling in mammalian cells with TurboID and split-TurboID. *Nat. Protoc.* 15, 3971–3999. doi: 10.1038/s41596-020-0399-0

Cornillez-Ty, C. T., Liao, L., Yates, J. R., Kuhn, P., and Buchmeier, M. J. (2009). Severe acute respiratory syndrome coronavirus nonstructural protein 2 interacts with a host protein complex involved in mitochondrial biogenesis and intracellular signaling. *J. Virol.* 83, 10314–10318. doi: 10.1128/JVI.00842-09

Coronado, L. M., Nadovich, C. T., and Spadafora, C. (2014). Malarial hemozoin: From target to tool. *Biochim. Biophys. Acta (BBA) - Gen. Subj.* 1840, 2032–2041. doi: 10.1016/j.bbagen.2014.02.009

Crosnier, C., Bustamante, L. Y., Bartholdson, S. J., Bei, A. K., Theron, M., Uchikawa, M., et al. (2011). Basigin is a receptor essential for erythrocyte invasion by *Plasmodium falciparum*. *Nature* 480, 534–537. doi: 10.1038/nature10606

Deans, A.-M., Nery, S., Conway, D. J., Kai, O., Marsh, K., and Rowe, J. A. (2007). Invasion pathways and malaria severity in Kenyan plasmodium falciparum clinical isolates. *Infect. Immun.* 75, 3014–3020. doi: 10.1128/IAI.00249-07

Emerson, V., Holtkotte, D., Pfeiffer, T., Wang, I.-H., Schnölzer, M., Kempf, T., et al. (2010). Identification of the cellular prohibitin 1/prohibitin 2 heterodimer as an interaction partner of the C-terminal cytoplasmic domain of the HIV-1 glycoprotein. *J. Virol.* 84, 1355–1365. doi: 10.1128/JVI.01641-09

Esser, C., Bachmann, A., Kuhn, D., Schuldt, K., Förster, B., Thiel, M., et al. (2014). Evidence of promiscuous endothelial binding by *Plasmodium falciparum*-infected erythrocytes. *Cell Microbiol.* 16, 701–708. doi: 10.1111/cmi.12270

Feire, A. L., Roy, R. M., Manley, K., and Compton, T. (2010). The glycoprotein B disintegrin-like domain binds beta 1 integrin to mediate cytomegalovirus entry. *J. Virol.* 84, 10026–10037. doi: 10.1128/JVI.00710-10

Fu, P., Yang, Z., and Bach, L. A. (2013). Prohibitin-2 binding modulates insulin-like growth factor-binding protein-6 (IGFBP-6)-induced rhabdomyosarcoma cell migration. *J. Biol. Chem.* 288, 29890–29900. doi: 10.1074/jbc.M113.510826

Galinski, M. R., Medina, C. C., Ingravallo, P., and Barnwell, J. W. (1992). A reticulocyte-binding protein complex of *Plasmodium vivax* merozoites. *Cell* 69, 1213–1226. doi: 10.1016/0092-8674(92)90642-P

Gaur, D., Singh, S., Singh, S., Jiang, L., Diouf, A., and Miller, L. H. (2007). Recombinant Plasmodium falciparum reticulocyte homology protein 4 binds to erythrocytes and blocks invasion. *Proc. Natl. Acad. Sci.* 104, 17789–17794. doi: 10.1073/pnas.0708772104

Graham, K. L., Halasz, P., Tan, Y., Hewish, M. J., Takada, Y., Mackow, E. R., et al. (2003). Integrin-Using Rotaviruses Bind $\alpha 2\beta 1$ Integrin $\alpha 2$ I Domain via VP4 DGE Sequence and Recognize $\alpha X\beta 2$ and $\alpha V\beta 3$ by Using VP7 during Cell Entry. *J. Virol.* 77, 9969–9978. doi: 10.1128/JV1.77.18.9969-9978.2003

Gruszczyk, J., Kanjee, U., Chan, L.-J., Menant, S., Malleret, B., Lim, N. T. Y., et al. (2018a). Transferrin receptor 1 is a reticulocyte-specific receptor for *Plasmodium vivax*. *Science* 359, 48–55. doi: 10.1126/science.aan1078

Gruszczyk, J., Lim, N. T. Y., Arnott, A., He, W.-Q., Nguitragool, W., Roobsoong, W., et al. (2016). Structurally conserved erythrocyte-binding domain in *Plasmodium* provides a versatile scaffold for alternate receptor engagement. *Proc. Natl. Acad. Sci. U.S.A.* 113, E191-200. doi: 10.1073/pnas.1516512113

Gupta, E. D., Anand, G., Singh, H., Chaddha, K., Bharti, P. K., Singh, N., et al. (2017). Naturally acquired human antibodies against reticulocyte-binding domains of plasmodium vivax proteins, pvRBP2c and pvRBP1a, exhibit binding-inhibitory activity. J. Infect. Dis. 215, 1558–1568. doi: 10.1093/infdis/jix170

HaileMariam, M., Eguez, R. V., Singh, H., Bekele, S., Ameni, G., Pieper, R., et al. (2018). S-trap, an ultrafast sample-preparation approach for shotgun proteomics. *J. Proteome Res.* 17, 2917–2924. doi: 10.1021/acs.jproteome.8b00505

Hallgren, J., Tsirigos, K. D., Pedersen, M. D., Almagro Armenteros, J. J., Marcatili, P., Nielsen, H., et al. (2022). DeepTMHMM predicts alpha and beta transmembrane proteins using deep neural networks. doi: 10.1101/2022.04.08.487609

Han, J.-H., Lee, S.-K., Wang, B., Muh, F., Nyunt, M. H., Na, S., et al. (2016). Identification of a reticulocyte-specific binding domain of *Plasmodium vivax* reticulocyte-binding protein 1 that is homologous to the PfRh4 erythrocyte-binding domain. *Sci. Rep.* 6, 26993. doi: 10.1038/srep26993

Horuk, R., Chitnis, C. E., Darbonne, W. C., Colby, T. J., Rybicki, A., Hadley, T. J., et al. (1993). A receptor for the malarial parasite *plasmodium vivax*: the erythrocyte chemokine receptor. *Science* 261, 1182–1184. doi: 10.1126/science.7689250

Kanjee, U., Grüring, C., Chaand, M., Lin, K.-M., Egan, E., Manzo, J., et al. (2017). CRISPR/Cas9 knockouts reveal genetic interaction between strain-transcendent erythrocyte determinants of *Plasmodium falciparum* invasion. *Proc. Natl. Acad. Sci. U.S.A.* 114, E9356–E9365. doi: 10.1073/pnas.1711310114

Kepple, D., Ford, C. T., Williams, J., Abagero, B., Li, S., Popovici, J., et al. (2023). Comparative transcriptomics reveal differential gene expression in *Plasmodium vivax* geographical isolates and implications on erythrocyte invasion mechanisms. *PLoS Negl. Trop. Dis.* 18, e0011926. doi: 10.1101/2023.02.16.528793

Kessler, A., Dankwa, S., Bernabeu, M., Harawa, V., Danziger, S. A., Duffy, F., et al. (2017). Linking EPCR-binding pfEMP1 to brain swelling in pediatric cerebral malaria. *Cell Host Microbe* 22, 601–614.e5. doi: 10.1016/j.chom.2017.09.009

Kuadkitkan, A., Wikan, N., Fongsaran, C., and Smith, D. R. (2010). Identification and characterization of prohibitin as a receptor protein mediating DENV-2 entry into insect cells. *Virology* 406, 149–161. doi: 10.1016/j.virol.2010.07.015

Lee, Y., Wiriyasermkul, P., Jin, C., Quan, L., Ohgaki, R., Okuda, S., et al. (2019). Cryo-EM structure of the human L-type amino acid transporter 1 in complex with glycoprotein CD98hc. *Nat. Struct. Mol. Biol.* 26, 510–517. doi: 10.1038/s41594-019-0237-7

Lex, A., Gehlenborg, N., Strobelt, H., Vuillemot, R., and Pfister, H. (2014). UpSet: visualization of intersecting sets. *IEEE Trans. Visual. Comput. Graphics* 20, 1983–1992. doi: 10.1109/TVCG.2014.2346248

Maginnis, M. S., Forrest, J. C., Kopecky-Bromberg, S. A., Dickeson, S. K., Santoro, S. A., Zutter, M. M., et al. (2006). Beta1 integrin mediates internalization of mammalian reovirus. *J. Virol.* 80, 2760–2770. doi: 10.1128/JVI.80.6.2760-2770.2006

Malleret, B., El Sahili, A., Tay, M. Z., Carissimo, G., Ong, A. S. M., Novera, W., et al. (2021). *Plasmodium vivax* binds host CD98hc (SLC3A2) to enter immature red blood cells. *Nat. Microbiol.* 6, 991–999. doi: 10.1038/s41564-021-00939-3

Malleret, B., Li, A., Zhang, R., Tan, K. S. W., Suwanarusk, R., Claser, C., et al. (2015a). Plasmodium vivax: restricted tropism and rapid remodeling of CD71-positive reticulocytes. *Blood* 125, 1314–1324. doi: 10.1182/blood-2014-08-596015

Matulis, D. (2016). Selective precipitation of proteins. CP Protein Sci. 83, 4.5.1-4.5.37. doi: 10.1002/0471140864.ps0405s83

Molina-Franky, J., Patarroyo, M. E., Kalkum, M., and Patarroyo, M. A. (2022). The cellular and molecular interaction between erythrocytes and *plasmodium falciparum* merozoites. *Front. Cell. Infect. Microbiol.* 12. doi: 10.3389/fcimb.2022.816574

Nägele, V., Heesemann, J., Schielke, S., Jiménez-Soto, L. F., Kurzai, O., and Ackermann, N. (2011). Neisseria meningitidis adhesin NadA targets beta1 integrins: functional similarity to Yersinia invasin. *J. Biol. Chem.* 286, 20536–20546. doi: 10.1074/jbc.M110.188326

Nguyen, N. N. T., Lim, Y.-S., Nguyen, L. P., Tran, S. C., Luong, T. T. D., Nguyen, T. T. T., et al. (2018). Hepatitis C Virus Modulates Solute carrier family 3 member 2 for Viral Propagation. *Sci. Rep.* 8, 15486. doi: 10.1038/s41598-018-33861-6

Ntumngia, F. B., Thomson-Luque, R., Galusic, S., Frato, G., Frischmann, S., Peabody, D. S., et al. (2018). Identification and immunological characterization of the ligand domain of *plasmodium vivax* reticulocyte binding protein 1a. *J. Infect. Dis.* 218, 1110–1118. doi: 10.1093/infdis/jiy273

Okuno, Y., Suzuki, A., Ichiba, S., Takahashi, T., Nakamura, K., Hitomi, K., et al. Establishment of an erythroid cell line (JK-1) that spontaneously diferentiates to red cells. *Cancer* 66, 544–1551. doi: 10.1002/1097-0142(19901001)66:7<1544::aid-cncr2820660719>3.0.co;2-9

Olaya-Galán, N. N., Salas-Cárdenas, S. P., Rodriguez-Sarmiento, J. L., Ibáñez-Pinilla, M., Monroy, R., Corredor-Figueroa, A. P., et al. (2021). Risk factor for breast cancer development under exposure to bovine leukemia virus in Colombian women: A case-control study. *PloS One* 16, e0257492. doi: 10.1371/journal.pone.0257492

Omasits, U., Ahrens, C. H., Müller, S., and Wollscheid, B. (2014). Protter: interactive protein feature visualization and integration with experimental proteomic data. *Bioinformatics* 30, 884–886. doi: 10.1093/bioinformatics/btt607

Pandey, A. V., and Tekwani, B. L. (1996). Formation of haemozoin/ β -haematin under physiological conditions is not spontaneous. *FEBS Lett.* 393, 189–192. doi: 10.1016/0014-5793(96)00881-2

Picón-Jaimes, Y. A., Lozada-Martinez, I. D., Orozco-Chinome, J. E., Molina-Franky, J., Acevedo-Lopez, D., Acevedo-Lopez, N., et al. (2023). Relationship between duffy genotype/phenotype and prevalence of *plasmodium vivax* infection: A systematic review. *TropicalMed* 8, 463. doi: 10.3390/tropicalmed8100463

Pierleoni, A., Martelli, P. L., and Casadio, R. (2008). PredGPI: a GPI-anchor predictor. BMC Bioinf. 9, 392. doi: 10.1186/1471-2105-9-392

Radoshitzky, S. R., Abraham, J., Spiropoulou, C. F., Kuhn, J. H., Nguyen, D., Li, W., et al. (2007). Transferrin receptor 1 is a cellular receptor for New World haemorrhagic fever arenaviruses. *Nature* 446, 92–96. doi: 10.1038/nature05539

Radoshitzky, S. R., Kuhn, J. H., Spiropoulou, C. F., Albariño, C. G., Nguyen, D. P., Salazar-Bravo, J., et al. (2008). Receptor determinants of zoonotic transmission of New World hemorrhagic fever arenaviruses. *Proc. Natl. Acad. Sci. U.S.A.* 105, 2664–2669. doi: 10.1073/pnas.0709254105

Rangel, G. W., Clark, M. A., Kanjee, U., Lim, C., Shaw-Saliba, K., Menezes, M. J., et al. (2018). Enhanced ex vivo *Plasmodium vivax* Intraerythrocytic Enrichment and Maturation for Rapid and Sensitive Parasite Growth Assays. *Antimicrob. Agents Chemother.* 62, e02519–e02517. doi: 10.1128/AAC.02519-17

Rathore, S., Dass, S., Kandari, D., Kaur, I., Gupta, M., and Sharma, Y. D. (2017). Basigin interacts with *plasmodium vivax*Tryptophan-rich antigen pvTRAg38 as a second erythrocyte receptor to promote parasite growth. *J. Biol. Chem.* 292, 462–476. doi: 10.1074/jbc.M116.744367

Rayner, J. C., Galinski, M. R., Ingravallo, P., and Barnwell, J. W. (2000). Two Plasmodium falciparum genes express merozoite proteins that are related to Plasmodium vivax and Plasmodium yoelii adhesive proteins involved in host cell selection and invasion. *Proc. Natl. Acad. Sci.* 97, 9648–9653. doi: 10.1073/pnas.160469097

Rayner, J. C., Vargas-Serrato, E., Huber, C. S., Galinski, M. R., and Barnwell, J. W. (2001). A *Plasmodium falciparum* Homologue of *Plasmodium vivax* Reticulocyte Binding Protein (PvRBP1) Defines a Trypsin-resistant Erythrocyte Invasion Pathway. *J. Exp. Med.* 194, 1571–1582. doi: 10.1084/jem.194.11.1571

Reyes, C., Picón Jaimes, Y. A., Kalkum, M., and Patarroyo, M. A. (2022). The Black Box of Cellular and Molecular Events of *Plasmodium vivax* Merozoite Invasion into Reticulocytes. *IJMS* 23, 14528. doi: 10.3390/ijms232314528

Ryan, J. R., Stoute, J. A., Amon, J., Dunton, R. F., Mtalib, R., Koros, J., et al. (2006). Evidence for transmission of *Plasmodium vivax* among a duffy antigen negative population in Western Kenya. *Am. J. Trop. Med. Hyg* 75, 575–581. doi: 10.4269/ajtmh.2006.75.575

Satchwell, T. J., Wright, K. E., Haydn-Smith, K. L., Sánchez-Román Terán, F., Moura, P. L., Hawksworth, J., et al. (2019). Genetic manipulation of cell line derived reticulocytes enables dissection of host malaria invasion requirements. *Nat. Commun.* 10, 3806. doi: 10.1038/s41467-019-11790-w

Smith, J. D., Kyes, S., Craig, A. G., Fagan, T., Hudson-Taylor, D., Miller, L. H., et al. (1998). Analysis of adhesive domains from the A4VAR Plasmodium falciparum erythrocyte membrane protein-1 identifies a CD36 binding domain. *Mol. Biochem. Parasitol.* 97, 133–148. doi: 10.1016/S0166-6851(98)00145-5

Snounou, G., Viriyakosol, S., Zhu, X. P., Jarra, W., Pinheiro, L., Do Rosario, V. E., et al. (1993). High sensitivity of detection of human malaria parasites by the use of nested polymerase chain reaction. *Mol. Biochem. Parasitol.* 61, 315–320. doi: 10.1016/0166-6851(93)90077-B

Su, W., Huang, S., Zhu, H., Zhang, B., and Wu, X. (2020). Interaction between PHB2 and enterovirus A71 VP1 induces autophagy and affects EV-A71 infection. *Viruses* 12, 414. doi: 10.3390/v12040414

Tailor, C. S., Nouri, A., Zhao, Y., Takeuchi, Y., and Kabat, D. (1999). A sodium-dependent neutral-amino-acid transporter mediates infections of feline and baboon

endogenous retroviruses and simian type D retroviruses. J. Virol. 73, 4470–4474. doi: 10.1128/JVI.73.5.4470-4474.1999

Tebben, K., Dia, A., and Serre, D. (2022). Determination of the stage composition of *plasmodium* infections from bulk gene expression data. *mSystems* 7, e00258–e00222. doi: 10.1128/msystems.00258-22

Teufel, F., Almagro Armenteros, J. J., Johansen, A. R., Gíslason, M. H., Pihl, S. I., Tsirigos, K. D., et al. (2022). Signal P 6.0 predicts all five types of signal peptides using protein language models. *Nat. Biotechnol.* 40, 1023–1025. doi: 10.1038/s41587-021-01156-3

Trager, W., and Jensen, J. B. (1976). Human malaria parasites in continuous culture. *Science* 193, 673–675. doi: 10.1126/science.781840

Trakarnsanga, K., Griffiths, R. E., Wilson, M. C., Blair, A., Satchwell, T. J., Meinders, M., et al. (2017). An immortalized adult human erythroid line facilitates sustainable and scalable generation of functional red cells. *Nat. Commun.* 8, 14750. doi: 10.1038/ncomms14750

Triglia, T., Thompson, J., Caruana, S. R., Delorenzi, M., Speed, T., and Cowman, A. F. (2001). Identification of Proteins from Plasmodium falciparum That Are Homologous to Reticulocyte Binding Proteins in Plasmodium vivax. *Infect. Immun.* 69, 1084–1092. doi: 10.1128/IAI.69.2.1084-1092.2001

Urquiza, M., Patarroyo, M., Marí, V., Ocampo, M., Suarez, J., Lopez, R., et al. (2002). Identification and polymorphism of *Plasmodium vivax* RBP-1 peptides which bind specifically to reticulocytes. *Peptides* 23, 2265–2277. doi: 10.1016/S0196-9781(02) 00267-X

Vigan-Womas, I., Guillotte, M., Juillerat, A., Hessel, A., Raynal, B., England, P., et al. (2012). Structural basis for the ABO blood-group dependence of *plasmodium falciparum* rosetting. *PloS Pathog.* 8, e1002781. doi: 10.1371/journal.ppat.1002781

Vogt, A. M., Barragan, A., Chen, Q., Kironde, F., Spillmann, D., and Wahlgren, M. (2003). Heparan sulfate on endothelial cells mediates the binding of *Plasmodium falciparum*–infected erythrocytes via the DBL1 α domain of PfEMP1. *Blood* 101, 2405–2411. doi: 10.1182/blood-2002-07-2016

Weigel-Kelley, K. A., Yoder, M. C., and Srivastava, A. (2003). $\alpha 5\beta 1$ integrin as a cellular coreceptor for human parvovirus B19: requirement of functional activation of $\beta 1$ integrin for viral entry. *Blood* 102, 3927–3933. doi: 10.1182/blood-2003-05-1522

Wintachai, P., Wikan, N., Kuadkitkan, A., Jaimipuk, T., Ubol, S., Pulmanausahakul, R., et al. (2012). Identification of prohibitin as a Chikungunya virus receptor protein. *J. Med. Virol.* 84, 1757–1770. doi: 10.1002/jmv.23403

World Health Organization (2024). World malaria report 2024: addressing inequity in the global malaria response. Geneva: World Health Organization. Licence: CC BY-NC-SA 3.0 IGO, ISBN 978-92-4-010444-0 (electronic version), ISBN 978-92-4-010445-7 (print version)

Xiao, J., Palefsky, J. M., Herrera, R., Berline, J., and Tugizov, S. M. (2008). The Epstein–Barr virus BMRF-2 protein facilitates virus attachment to oral epithelial cells. *Virology* 370, 430–442. doi: 10.1016/j.virol.2007.09.012

Yan, R., Zhao, X., Lei, J., and Zhou, Q. (2019). Structure of the human LAT1-4F2hc heteromeric amino acid transporter complex. *Nature* 568, 127–130. doi: 10.1038/s41586-019-1011-z

Yipp, B. G., Anand, S., Schollaardt, T., Patel, K. D., Looareesuwan, S., and Ho, M. (2000). Synergism of multiple adhesion molecules in mediating cytoadherence of *Plasmodium falciparum*-infected erythrocytes to microvascular endothelial cells under flow. *Blood* 96, 2292–2298. doi: 10.1182/blood.V96.6.2292

Yoshimoto, T., Yoshimoto, E., and Meruelo, D. (1993). Identification of amino acid residues critical for infection with ecotropic murine leukemia retrovirus. *J. Virol.* 67, 1310–1314. doi: 10.1128/jvi.67.3.1310-1314.1993

Yu, F., Haynes, S. E., and Nesvizhskii, A. I. (2021). IonQuant enables accurate and sensitive label-free quantification with FDR-controlled match-between-runs. *Mol. Cell. Proteomics* 20, 100077. doi: 10.1016/j.mcpro.2021.100077